

Beyond Trial and Error: A Systematic Development of Liposomes Targeting Primary Macrophages

Florian Weber, Daniela C. Ivan, Steven T. Proulx, Giuseppe Locatelli, Simone Aleandri,* and Paola Luciani*

Monocytes/macrophages are phagocytic innate immune cells playing a pivotal role in tissue homeostasis, inflammation, and antitumor immunity in a microenvironment-dependent manner. By expressing pattern recognition and scavenger receptors on their surface, macrophages selectively take up pathogens, cellular debris, and often—undesirably—drug delivery systems. On the other hand, the propensity of phagocytic cells to internalize particulate drug carriers is used to load them with a cargo of choice, turning the monocytes/macrophages into a diagnostic or therapeutic Trojan horse. Identifying the ideal physico-chemical properties of particulate carriers such as liposomes to achieve the most efficient macrophage-mediated drug delivery has been object of extensive research in the past, but the studies reported so far rely solely on trial-and-error approaches. Herein, a design of experiment (DoE) strategy to identify the optimal liposomal formulation is proposed, fully characterized in terms of size, surface charge, and membrane fluidity, to maximize macrophage targeting. The findings are validated using mouse bone marrow-derived macrophages, a primary preparation modeling in vivo monocyte-derived macrophages, thus confirming the robustness and versatility of the systematic and iterative approach and suggesting the promising potential of the DoE approach for the design of cell-targeting delivery systems.

in regulating tissue homeostasis, inflammation, and antitumor immunity in a microenvironment-dependent manner.^[1] Their distinct transcriptional plasticity allows these cells to integrate local and systemic cues and exert a continuous spectrum of functions, ranging from tissue damage to wound healing. Thanks to the ability of monocytes to infiltrate inflamed tissues and differentiate into monocyte-derived macrophages (MdMs), monocytes have also been exploited as a drug delivery target in a broad range of pathologies spanning from cancer to Alzheimer's and Parkinson's disease.^[2] Due to their surface expression of pattern recognition and scavenger receptors (SRs), macrophages selectively take up pathogens and cellular debris,^[3] a property that can be utilized for cell-specific drug targeting. It was successfully demonstrated that the decoration of the surface of nanocarriers with ligands such as antibodies, mono- and polysaccharides, and lectins resulted in an increased macrophage uptake.^[4] Remarkable preclinical success has been obtained using


1. Introduction

Monocytes/macrophages are phagocytic innate immune cells populating every organ of the body and playing a pivotal role

liposomes,^[5–8] which exhibit low toxicity and whose lipid composition can be modified to control physical and chemical properties such as fluidity and surface charge. Specific macrophage targeting is obtained by fine tuning liposome characteristics such as lipid composition,^[9] size, and surface charge.^[4,10] Engineered vesicles with negatively charged phospholipids (NPLs), such as phosphatidylserine (PS), have received growing interest for their ability to be engulfed by macrophages through SR-mediated endocytosis.^[4] Under physiological conditions, PS is preferentially located on the inner leaflet of eukaryotic plasma membrane and in endocytic membranes, whereas phosphocholine (PC) resides more commonly in the outer leaflet. However, this asymmetrical arrangement is altered when cells undergo apoptosis when PS is exposed on the outer leaflet of the membrane, a phenomenon that also occurs during non-apoptotic cell death.^[11] The exposure of the PS domain on the cell surface via the action of scramblases provokes a so-called eat-me-signal responsible for the initiation of intracellular signaling cascades, cytoskeletal rearrangement, and debris engulfment by macrophages.^[12,13] PS is one of the best characterized membrane-anchored eat-me signals and its recognition is a stereo-specific process: only L-phosphoserine is

Dr. F. Weber, Dr. S. Aleandri, Prof. P. Luciani
Department of Chemistry
Biochemistry and Pharmaceutical Sciences
University of Bern
Bern 3012, Switzerland
E-mail: simone.aleandri@dcb.unibe.ch; paola.luciani@dcb.unibe.ch

D. C. Ivan, Dr. S. T. Proulx, Dr. G. Locatelli
Theodor Kocher Institute
University of Bern
Bern 3012, Switzerland

 The ORCID identification number(s) for the author(s) of this article can be found under <https://doi.org/10.1002/anbr.202000098>.

© 2021 The Authors. Advanced NanoBiomed Research published by Wiley-VCH GmbH. This is an open access article under the terms of the Creative Commons Attribution License, which permits use, distribution and reproduction in any medium, provided the original work is properly cited.

DOI: 10.1002/anbr.202000098

recognized and engulfed either as a mere lipid or in combination with other soluble proteins.^[14]

Furthermore, phosphatidylglycerol (PG), as a major component of Gram-negative bacterial cell membranes, represents an essential ligand for different phagocytes.^[15] PG-based liposomes have shown anti-inflammatory activities in a recent *in vitro* study with decreased TNF α -production of lipopolysaccharide-stimulated mouse peritoneal macrophages.^[16] Other headgroups, such as phosphatic acid (PA), with a crucial role in vesicle trafficking and endocytosis,^[17] have been shown to be taken up by alveolar macrophages upon administration of PA-based liposomal aerosols *in vivo*. Finally, given the high expression of mannose receptors (MRs) in most tissue-resident macrophages and certain MdMs, mannoseylated liposomes have also demonstrated efficient macrophage targeting, both *in vitro* and *in vivo*.^[18,19]

Despite the manifold literature available addressing the correlation between macrophage uptake and physicochemical properties of carrier formulation, trial-and-error approaches to target macrophages are still the predominant modality in small-scale production. In academia and in laboratory-scale product development, the proclivity to test as many formulations as possible to ultimately identify a suitable candidate for further evaluation (Quality by Testing) is indeed a deeply-rooted—albeit often inefficient—philosophy.^[9] In contrast, the risk-minimizing pharmaceutical Quality by Design (QbD) approach proposes to evaluate a formulation and the corresponding manufacturing process through its key material attributes and process parameters and, aided by the gained information and a sound risk assessment, can improve the understanding of the formulation and the process over the product lifecycle.^[20] A fundamental aspect of QbD is the use of a design of experiment (DoE) strategy to screen the range of formulation parameters that have been demonstrated to provide assurance of quality. The DoE approach uses a rational and statistically validated method that designs the number of experiments depending on the parameters to be optimized while providing insights into the decision-making process, as recommended by the FDA (FDA 2007; ICH Q8 guidelines). The implementation of a DoE approach has been increasingly used to develop formulations for a wide range of dosage forms including liposomes, micelles, dendrimers, polymeric nanoparticles, and microparticles.^[21–24] Recently, a DoE approach was used to estimate the macrophage sequestration of liposomes functionalized with different poly(ethylene) glycols (PEGs) in zebrafish embryos.^[25] Different from what is proposed in the majority of the available literature, we conceived the present study relying on a systematic approach that would enable the examination of several variables at the same time and the correlation of the liposomal properties to macrophage targeting. Our driving hypothesis was that by selecting and combining different lipids, the features of the derived nanomaterial by design would be affected, thereby providing control over liposome uptake. Accordingly, four independent DoEs, where the neutral lipids (1,2-dioleoyl-sn-glycero-3-phosphocholine [DOPC], 1-palmitoyl-2-oleoyl-glycero-3-phosphocholine [POPC], 1,2-dipalmitoyl-sn-glycero-3-phosphocholine [DPPC], and DOPC + 1,2-distearoyl-sn-glycero-3-phosphocholine [DSPC] 50/50 mixture) were formulated together with negatively charged lipids (1,2-dioleoyl-sn-glycero-3-phospho-L-serine [DOPS], 1-hexadecanoyl-2-(9Z-octadecenoyl)-sn-glycero-3-phospho-L-serine

[POPS], 1,2-dipalmitoyl-sn-glycero-3-phospho-L-serine (DPPS), and L-alpha-PS from brain [Brain PS], respectively) and cholesterol (Chol), were carried out. Once the optimal lipid proportion and composition to maximize uptake were found, the types of NPLs and the liposome size were varied stepwise as well.

In initial screenings, the RAW264.7 mouse cell line was used as a widely acknowledged monocyte/macrophage model typically in *in vitro* liposome phagocytosis assays. However, RAW264.7 cells are an immortalized model that does not fully resemble the physiological phagocytosis observed in *ex vivo* macrophages.^[26] As a systematic comparison between liposome uptake by RAW264.7 cells and by primary macrophages is missing to date, we aimed at further confirmation of our findings using mouse bone marrow-derived macrophages (BMDMs), a primary preparation often used to model the properties of tissue-resident macrophages or inflammatory MdMs depending on the specific experimental scenario.^[27] Our systematic approach guided us to the identification of a liposomal formulation specifically, efficiently taken up by RAW264.7 cells. The optimal candidate from QbD screening also exhibited similar uptake by BMDMs, thus validating the robustness and versatility of our iterative procedure in the formulation optimization for cell targeting and suggesting the translational potential of a DoE design for subsequent *in vivo* studies.

2. Results and Discussion

Fine tuning liposome properties such as size, surface, and bilayer rigidity is crucial to determine if and how macrophages can internalize a therapeutic cargo.^[28] The proposed investigation is built on a DoE approach which allows us to simultaneously alter either the lipid composition or the lipid proportions and observe how these changes affect the chosen outcome, in our case macrophage uptake. Four independent DoEs were conducted, in which the neutral lipids were formulated together with Chol and negatively charged PS, as the inclusion of PS in formulations represents a reference procedure when aiming for phagocytosis in therapeutic formulations.^[29–34] Once the optimal proportion between the components (neutral, Chol, and PS) was found and the best candidate between the four DoEs selected, the headgroup of the NPL and the size of liposomes were varied stepwise and their uptake evaluated using the RAW264.7 cell line and primary BMDMs.

2.1. Varying the Liposome Formulation: Effect of the Lipid Chain and Cholesterol

To ensure that the obtained differences in uptake were not dependent on formulation variability, all produced liposomes were first fully characterized in terms of size, zeta potential, and molar percentages of each lipid in the formulations. As expected, the zeta potential and the particle size were similar for each set of experiments between the liposomes containing the same NPL, whereas the particle charge decreased as the percentage of NPL increased (**Figure 1A,B**). The molar percentages of each lipid in the liposomal formulations after preparation were not divergent from the theoretical values (see **Figure S7**, Supporting Information) and all the produced formulations were

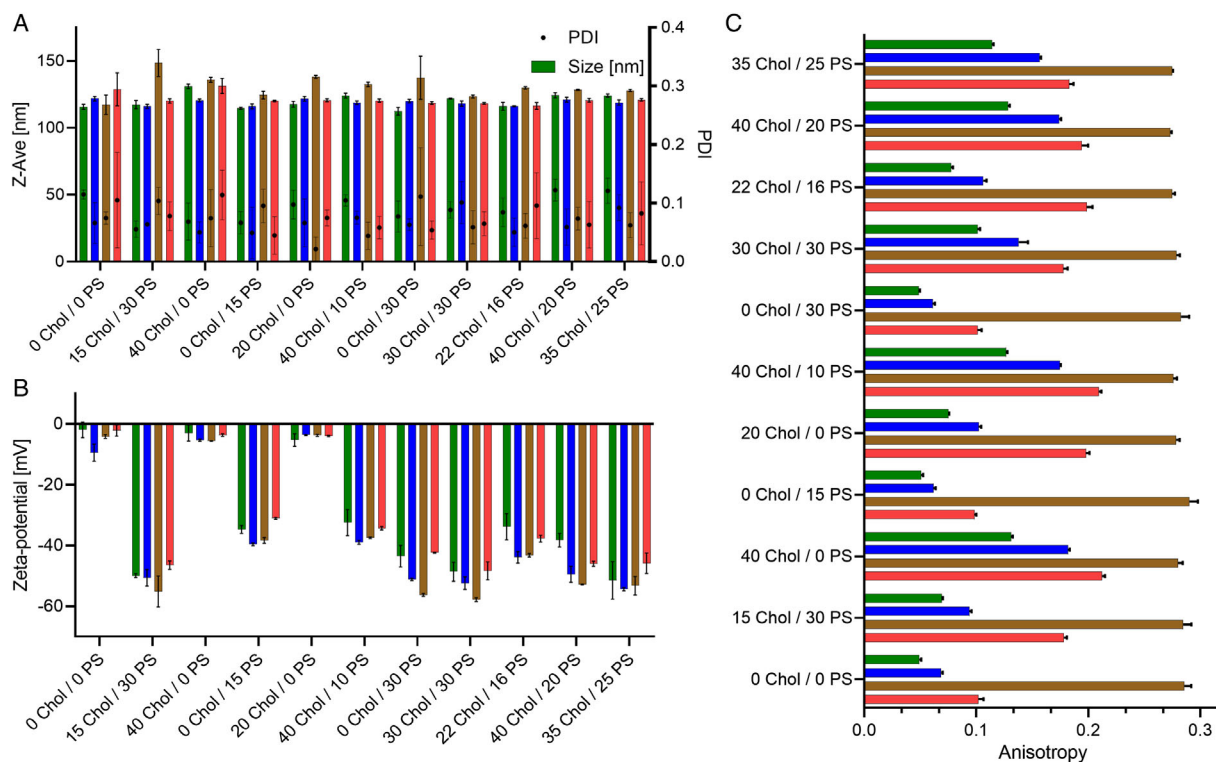


Figure 1. A) Size and PDI, B) zeta potential, and C) anisotropy, for the DOPX (DOPC-based liposomes containing different amount of PS and Chol; green bars), POPX (POPC-based liposomes containing different amount of PS and Chol; blue bars), DPPX (DPPC-based liposomes containing different amount of PS and Chol; brown bars), and Brain PX series (DOPC/DSPC-based liposomes containing different amount of PS and Chol; red bars). Data are represented as mean \pm SD ($n = 3$).

stable over 1 month (See Figure S8 and S9, Supporting Information).

To correlate the characteristics of the lipid chain with the macrophage uptake, the anisotropy (r) of the liposomes was determined as a measure of the membrane motional fluidity.

A shorter chain length and the introduction of cis double bonds in the acyl chains are reported to be responsible for a decreased phase transition temperature (T_m), which in turn causes reduced rigidity and lower anisotropy.^[35] Interestingly, DOPC-based liposomes, containing either different amounts of PS or Chol (DOPX series) with the lowest anisotropy value (Figure 1C), showed the highest uptake by RAW264.7 cells with respect to the other lipids at 37 °C (Figure 2A), whereas the DOPC/DSPC- and the POPC-based liposomes (Brain PX and POPX series, respectively) with intermediate anisotropy values showed the second- and third-highest uptake (3.3-fold and 4.8-fold lower than DOPC, respectively).

DPPC liposomes (DPPX series), having a T_m (41 °C) higher than physiological temperature, are the most rigid, and showed the poorest uptake by RAW264.7 cells (6.4-fold lower than DOPC). Although these results suggest that the fluidity of the acyl chain contributes to particle uptake, a direct correlation between those two parameters was not possible: despite the fact that POPC liposomes have a lower anisotropy than the DOPC/DSPC mixture, the latter formulation was taken up to a higher extent. POPC/POPS-based liposomes which modulate various

cellular signaling pathways have been already used to reprogram macrophages,^[36] and POPC is responsible for the activation of alveolar macrophages and regulating their production of cytokines.^[37] However, the liposomal effect was attributed mainly to the presence of PS, whereas a comparison with other PC-based liposomes and the lipid chain contribution on the uptake has so far been completely missing. Herein, the superior uptake of DOPC/DSPC mixture (Brain PX series) may be attributed to the fully unsaturated DOPC domain in the formulations, which is the predominant lipid determining the interaction with the cellular membrane, resulting in elevated endocytosis.^[38–42] Therefore, it became apparent that the lipid chain fluidity of the formulation should not be the only parameter evaluated and that other variables should be considered when correlating the liposomal features with their uptake. The incorporation of Chol in the liposomal membrane is widely used to modulate membrane fluidity and therefore vesicle stability.^[37–39]

However, the influence of Chol on liposome uptake is elusive and the reported publications are limited and inconsistent.^[10,41,43–50] However in some studies the inclusion of Chol was observed to enhance immune responses, other investigations have demonstrated that liposomes containing Chol showed decreased adjuvant effects. For example, Jiskoot and coworkers demonstrated a significantly elevated uptake by dendritic cells after the incubation with Chol-containing liposomes compared with Chol-free vesicles.^[51] In addition, successful phagocytic cell

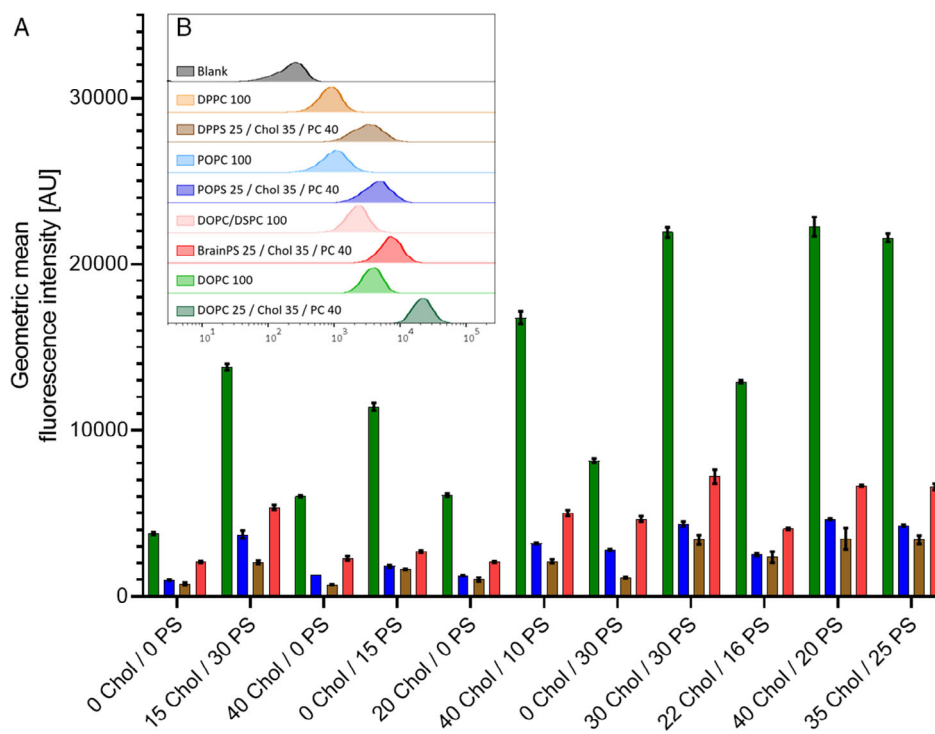


Figure 2. A) Geometric mean of the fluorescence intensity of RAW264.7 cells after incubation with formulations composed of DOPX (green bars), POPX (blue bars), DPPX (brown bars), and Brain PX series (red bars). PS: The corresponding phosphatidylserine. Data are represented as mean \pm SD ($n = 3$). B) Representative histograms of the formulations with the highest and the lowest uptake for each set of experiments in comparison with the blank (untreated cells).

uptake using PS-liposomes with 32 mol% Chol has been shown, suggesting the importance of this excipient in macrophage-targeting applications.^[31] Conversely, it has been reported that the inclusion of Chol at a high percentage ($>50\%$), and thus augmented particle rigidity, resulted in a decreased uptake by macrophages.^[48]

As shown in Figure 2, Chol has a remarkable impact on the formulation uptake. The effect is especially evident in the evaluation of the series containing the same amount of PS (30 mol %) and different percentages of Chol: the Chol-free formulation results in a RAW264.7 uptake 2- and 4-fold lower than the liposomes containing 15 and 30 mol% Chol, respectively. It has been described that macrophages take up Chol-rich remnants of lipoproteins through low-density lipoprotein receptors, SRs of class B type I, and fluid-phase pinocytosis.^[49,50,52] Therefore, liposomes with a high cholesterol content, having adsorbed opsonizing proteins on their surface, appear to mimic natural chylomicrons and can thus be actively taken up by macrophages.

Nevertheless it has to be noted that in the case of PEGylated liposomes, of which the Chol-enriched surface is shielded by PEG chains, their opsonization is lower with respect to the non-PEGylated ones.^[14] However, it has been reported that although PEGylated liposomes are barely taken up by macrophages at the steady state, PEGylated liposomes display a preferential affinity for and a higher uptake from activated macrophages in inflammatory diseases such as arthritis.^[53]

In summary, the results of our DoE-led experiments, in agreement with the findings from other groups, strongly support the hypothesis that a high Chol content (40 ± 5 mol%) markedly contributes to an increased uptake of non-PEGylated liposomes by macrophages.

2.2. NPL Content

As already proposed by other authors, the statistical evaluation of our data by response optimization (Table S10–S13, Supporting Information) displays that the liposomal uptake by macrophages is a PS concentration-dependent phenomenon, and it reaches its maximum when the PS content is 25 ± 5 mol%.^[29,31,33] Until now, several receptors involved in PS-mediated uptake have been described including BAI1, Tim-1, Tim-2, Tim-4, Stabilin-2, CD300, and TREM2.^[54] Ouyang et al. described T-cell immunoglobulin mucin 4 (Tim-4) as a possible candidate for PS recognition.^[55] This receptor is normally expressed on the surface of macrophages and mediates binding to surrounding apoptotic bodies. After binding to PS, Tim-4 is also directly involved in the engulfment of particles. Moreover, a second possible pathway for the uptake of negatively charged liposomes is their aforementioned affinity to opsonizing proteins such as complement components or immunoglobulins in the presence of serum. Several groups have identified that these proteins can increase the interactions between the negatively charged liposomes and

macrophages.^[56–60] However, due to their variety, a comprehensive explanation of PS binding still remains unclear.

2.3. Statistical Evaluation and Model Analysis

The contour plots (Figure 3) summarize how the response (i.e., the liposome uptake, expressed as geometric mean fluorescence intensity values obtained from flow cytometry experiments) relates to lipid proportion. The graph provides a 2D view in which all points that have the same response are linked to produce contour lines of constant responses. Colored contour bands (which represent ranges of the response values) get darker if the uptake increases. To maximize this outcome, we had to choose the proportions for the components in the bottom center of the design space, where the ratings (i.e., the uptake) are the highest. It is also worth noting that, for all models, the association between the response and two-way interaction terms such as neutral lipids versus NPL or NPL versus Chol is statistically significant (Tables S2, S4, S6, and S8, Supporting Information). The response therefore is dependent on both terms and it increases as the neutral lipid decreases, whereas the NPL and Chol amount are increased at the same time, as visible from the contour plots. On the other hand, the association between the response and two-way interaction terms such as neutral lipids versus Chol is not statistically significant, meaning that the uptake is not affected by the interaction between Chol and neutral lipids. Moreover, the response optimization (Tables S10–S13,

Supporting Information) was used to identify the best lipid proportion able to maximize the macrophage uptake. Overall, our findings suggest that liposomes mainly composed of DOPC, independent of the proportions between the lipid components, result in the higher uptake by RAW264.7 cells with respect to the POPC-, DOPC/DPPS-, and the DPPC-based liposomes. The maximum uptake can be achieved with the formulation containing 40% of DOPC, 22% of DOPS, and 38% of Chol. The results are in line with those reported in literature, where DOPS/Chol-liposomes imply a 5.3-fold increase in uptake compared with neutral liposomes in a macrophage cell model.^[9] Moreover, these predicted results estimated by the analysis of mixture design are in agreement with those evaluated experimentally (See Table S10–S13, Supporting Information). Therefore, the proposed model is an easy approach for optimization of lipid mixtures of liposomes and it enables theoretical understanding of optimal liposome formulation.

2.4. Influence of the Headgroup

Starting from the best formulation obtained from the DoE analysis (40% of DOPC, 22% of DOPS, and 38% of Chol), the PS headgroup was replaced with glycerol (PG), PA, or mannose (Man) headgroups to assess if and how different surface moieties would influence the liposome/cell interactions. As earlier, all the vesicles were fully characterized (see Figure 4). They had similar fluorescent intensity and exhibited no differences in cell viability

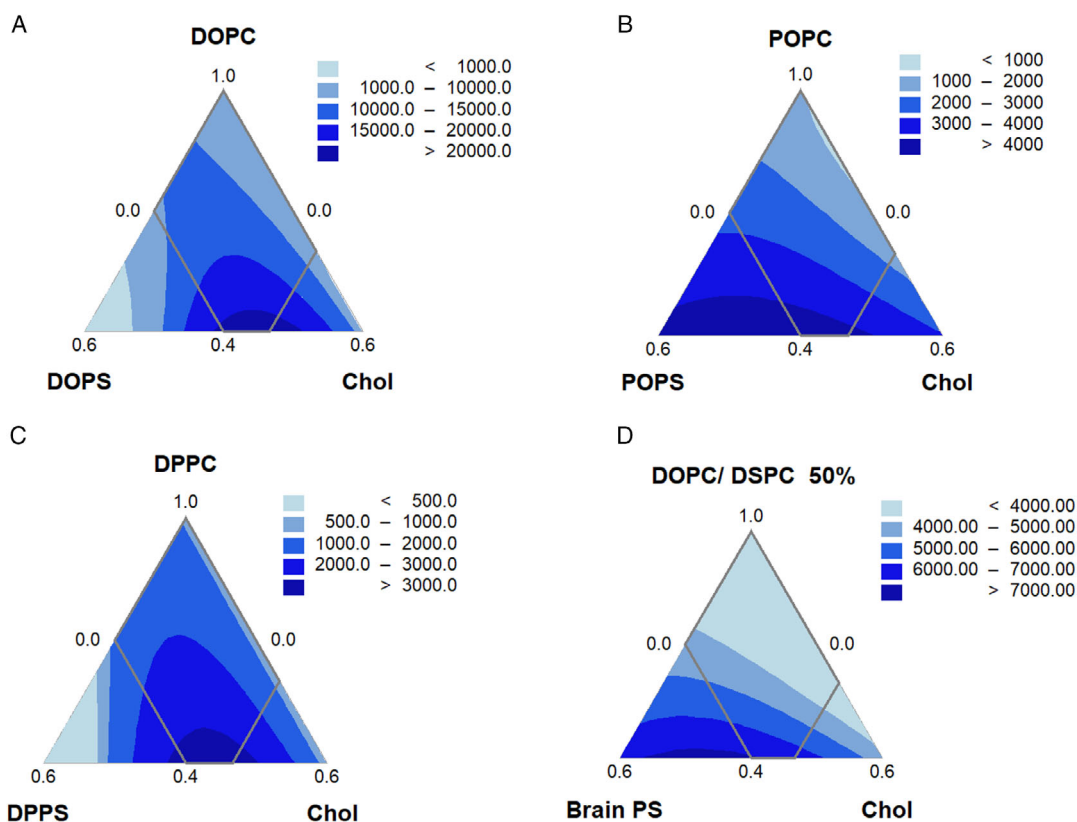


Figure 3. Response contour plot for the A–D) DOPX, POPX, DPPX, and Brain PX series (respectively). The colored contour bands show ranges of different geometric mean fluorescence intensity values obtained from flow cytometry experiments ($n = 3$).

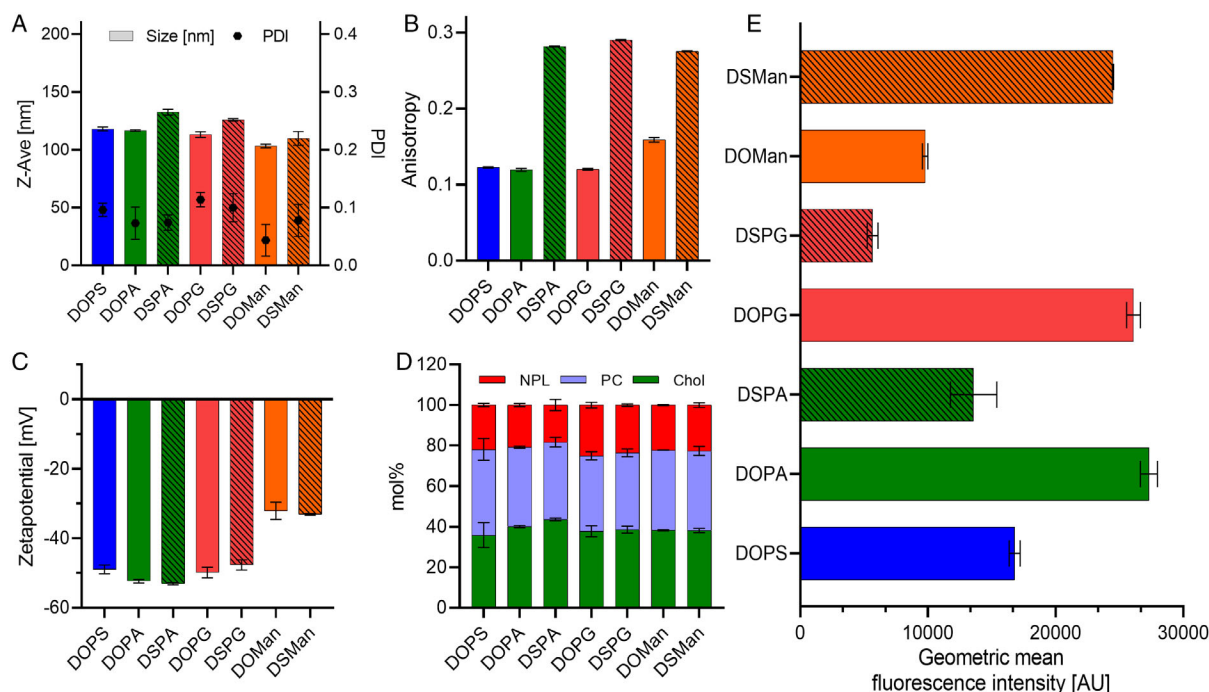


Figure 4. A) Size, B) anisotropy, C) zeta potential, D) UHPLC-CAD lipid quantification, and E) uptake into RAW264.7 cells for the different headgroup formulations. Data are represented as mean \pm SD ($n = 3$).

after incubation (See Figure S10 and S11, Supporting Information, respectively). Moreover, to correlate the uptake with the different NPLs used and ascertain that the difference in uptake values was only gained by the different headgroups, a comprehensive control with fully saturated formulations having the same chain length (DSPX, C18) was used. As shown in Figure 4, the liposomes were fully characterized in terms of lipid composition, surface charge, size, anisotropy, and cellular uptake. The differences in particle size and lipid content for all formulations were negligible, whereas the zeta potential of Man based-liposomes showed a less negative voltage (≤ -32 mV) due to the electrostatic shielding of the intramolecular PA induced by the mannose linked to triethyleneglycol, which is in agreement with what has been reported.^[61]

As expected, all unsaturated formulations were characterized by low anisotropy and therefore by high membrane fluidity with respect to their saturated counterparts.^[62] The minor difference in anisotropy of DOMan and DSMan compared with the other associated unsaturated or saturated formulations could be explained by the presence of a mannosylated lipid in the formulation, where a mannose polar headgroup is linked via PEGylated triazole with a dipalmitoyl chain. For the case of PA- and PG-based liposomes, the unsaturated formulations showed a superior uptake with respect to their saturated counterparts, which is in line with the results described earlier. An exception is given by the Man based-vesicles, whose saturated, thus more rigid, formulation was preferably taken up. A possible explanation could be found in the natural function of the MR (MR/CD206).^[63] MR is mostly responsible for binding and aiding the phagocytosis of mannose-linked microorganisms,^[64] with the majority of the natural receptor substrate mainly located on the surface of bacterial

cell walls characterized by a higher stiffness compared with mammalian cellular membranes.^[65]

As shown in Figure 4E, even though the PS-based liposomes represent one of the most used formulations to target macrophages,^[5,9,10] our results revealed that other headgroups, namely PA, PG, and Man, could lead to a higher macrophage uptake.

In agreement with our findings, Slütter and coworkers demonstrated that PG-containing liposomes mediated an increased antigen-specific immune cell response with respect to PS-containing liposomes.^[66] Moreover, PS-liposomes are mainly dependent on the SR, whereas PG-liposomes have at least one additional mechanism of uptake such as a Toll-like receptor 4 (TLR4)-dependent binding.^[67] Another explanation for the higher potency of PG-liposomes could be attributed to their increased affinity to the complement component 1q (C1q) compared with PS-liposomes. Furthermore, an opsonizing protein-independent pathway was observed after detecting an uptake of PG-liposomes in serum-free conditions.^[68]

Unfortunately, no satisfying data describing a potential uptake mechanism by macrophages are available for PA-containing liposomes. Yanasarn et al. demonstrated that DOPA-liposomes exhibited increased uptake with respect to pure DOPC liposomes in vitro and upregulated a specific immune response in vivo in the same manner as DOPS.^[68] Furthermore, PA increases the expression of major histocompatibility complex II (MHC II), a molecule expressed on the surface of phagocytes responsible for initiating antigen-specific immune responses.^[68] PA-liposomes are negatively charged in physiological pH and are therefore characterized by strong interactions with opsonizing proteins in a similar manner as PS liposomes.

The combination of a protein-corona-driven uptake due to the interaction with PA on the outer surface can additionally contribute to an elevated engulfment rate and immune response initiation.

DSMan liposomes exploit the MR expressed on the macrophage's surface (vide supra) and exhibit superior uptake with respect to plain liposomes.^[61] Despite being a promising candidate, the limited availability of mannosylated lipids on the market led us to the decision to exclude DSMan from further experiments. Our decision was further supported by the absence of a commercial unsaturated lipid functionalized with Man, a shortcoming that prevented us from establishing a direct correlation with other DOPC based-formulations.

The influence of different negatively charged headgroups on the uptake by macrophages is a controversial topic and the availability of related data is limited and has not been generated in a systematic fashion. To the best of our knowledge, only the ability of both PS- and PG-enriched liposomes to act as anti-inflammatory agents has been investigated,^[69] whereas no direct comparison between these phospholipid headgroups has been performed so far.

After examining the formulation, resulting in highest macrophage internalization, an additional test to investigate the liposomal uptake in a nonmacrophage cell line was conducted with the aim of evaluating the specificity of our formulation. The human embryonic kidney 293 cell line (HEK293) was chosen as a model for nonphagocytic cells without engulfment activity under normal conditions^[70] and used as negative control. After incubation with DOPC, DOPS, and DOPG liposomes, all particles were equally internalized (see Figure S12,

Supporting Information), indicating the remarkable specificity of PG and PS liposome toward macrophages.

2.5. Influence of the Particle Size

Another important and controversial parameter is the influence of the particle size on the uptake by macrophages.^[10,71] While it has been reported that mannose-^[72,73] and PS-based liposomes^[74] showed augmented uptake with increased size, other studies suggested an increased opsonization into macrophages for small negatively charged particles with ≈ 100 nm diameter.^[38,71,75] Perrie's group elucidated that positively charged liposomes showed comparable uptake in phagocytes regardless of particle size (200 nm–2 μ m) in vitro.^[76] The optimal size seems to be dependent on the charge (and composition) of the liposome, the cell line, and the targeted receptor mediating the uptake. In our set of experiments, we produced DOPA, DOPG, and DOPS liposomes of different sizes, as shown in **Figure 5A**. The differences in anisotropy, surface charge, and composition between the particles were negligible (**Figure 5B–D**), as well as the fluorescence intensity and the viability of the particles after incubation (See **Figure S13** and **S14**, Supporting Information), thus confirming that the prepared liposomes differed essentially only in size. As far as the uptake was concerned, a very clear pattern could be observed, showing that the uptake was inversely proportional to liposome size. The best outcome was detected for 100 nm DOPG particle size (see **Figure 5E**). Our results are in agreement with the literature, where liposomes formulated with negatively charged lipids (PS-based liposomes) with a size of 85 nm showed the best internalization

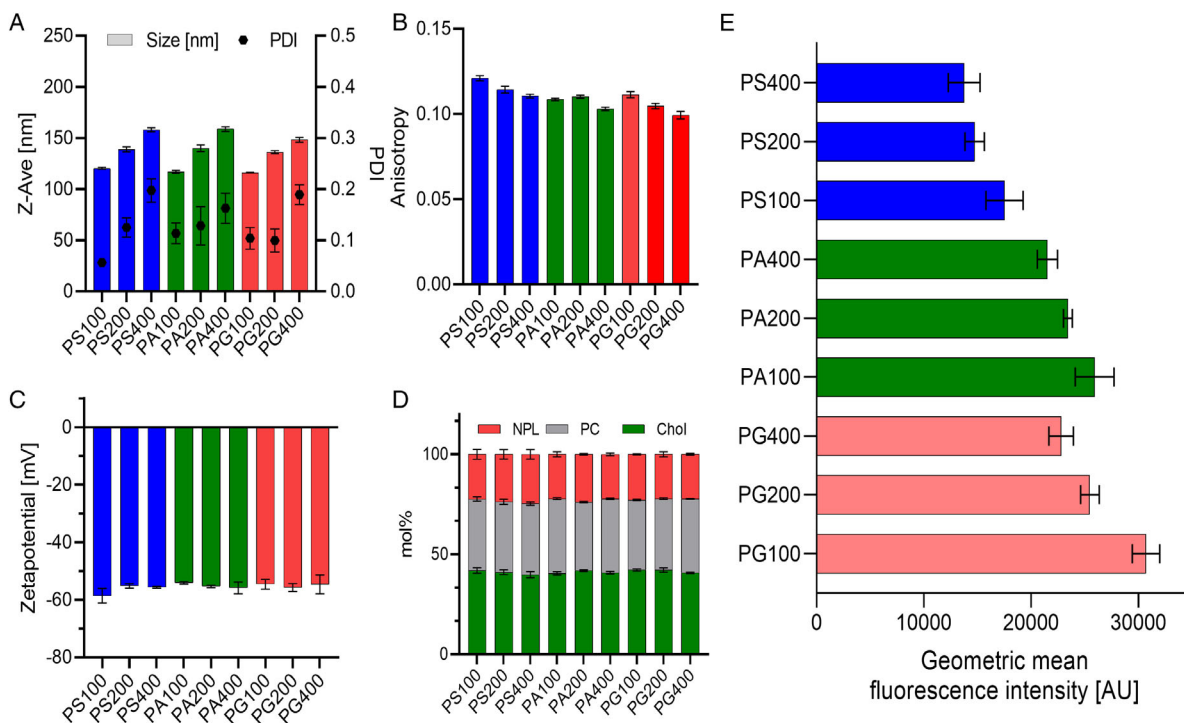


Figure 5. A) Size, B) anisotropy, C) zeta potential, D) UHPLC-CAD lipid quantification, and E) RAW264.7 uptake, for the different size liposomes formulated with DOPA, DOPG, and DOPS. Data are represented as mean \pm SD ($n = 3$).

rate into different cell lines.^[9,77] Ultimately, the formulation characterized by the highest uptake into macrophages contained 22 mol% of DOPG, 38 mol% of Chol, and 40 mol% of DOPC resulting in a size of 116.2 ± 0.2 nm.

2.6. Primary Mouse BMDM-Targeting Liposomes

Aiming to test the translational potential of our systematic screening approach, we thus moved to BMDMs, a more physiological cellular model obtained by in vitro differentiation of primary hematopoietic progenitors isolated from the bone marrow of mice and often used to model the characteristics of MdMs found in inflamed tissues. Although RAW264.7 is recognized widely as a monocyte/macrophage model, significant differences with BMDMs, such as varying expression levels of a large number of proteins including important receptors, are reported.^[26] Hence, we aimed to verify if the uptake obtained from the RAW264.7 cell line was comparable with that achieved by primary cells. The investigation was conducted using three formulations: 1) pure DOPC liposomes as a negative control, 2) DOPS-based liposomes as a positive control as PS is one of the most used membrane-anchored eat-me signals, and 3) DOPG

liposomes, which stood out as the best formulation taken up by RAW264.7 cells. The PS- or PG-based liposomes were both formulated with a diameter of 100 nm and each contained 22 mol% of NPL and 38 mol% of Chol. As evident from the confocal images (Figure 6, panel A and B) and confirmed quantitatively by flow cytometry (Figure 6, panel C and D), a similar trend was observed in both types of cells. As with RAW264.7 cells, the PG-based liposomes also showed the highest uptake by the BMDMs when compared with either the pure DOPC or the “gold standard” PS-based liposomes. Therefore, the ability of the PG candidate to be taken up by BMDMs in a similar manner as by RAW264.7 cells was confirmed, thus validating the robustness and versatility of our iterative procedure in the optimization of formulations for cell targeting. As in the case of RAW264.7 cells, the phagocytic affinity of BMDMs for PG-based liposomes could be explained by an SR-independent pathway for PG-containing particles. Whereas PS liposomes are mainly dependent on SRs function for uptake, PG liposomes could be engulfed via at least one additional mechanism of uptake^[66] and very likely the observed uptake is mediated by several receptors/molecules including SRs. Moreover, it has been shown that a higher serum protein-binding capacity of DOPG liposomes is correlated with

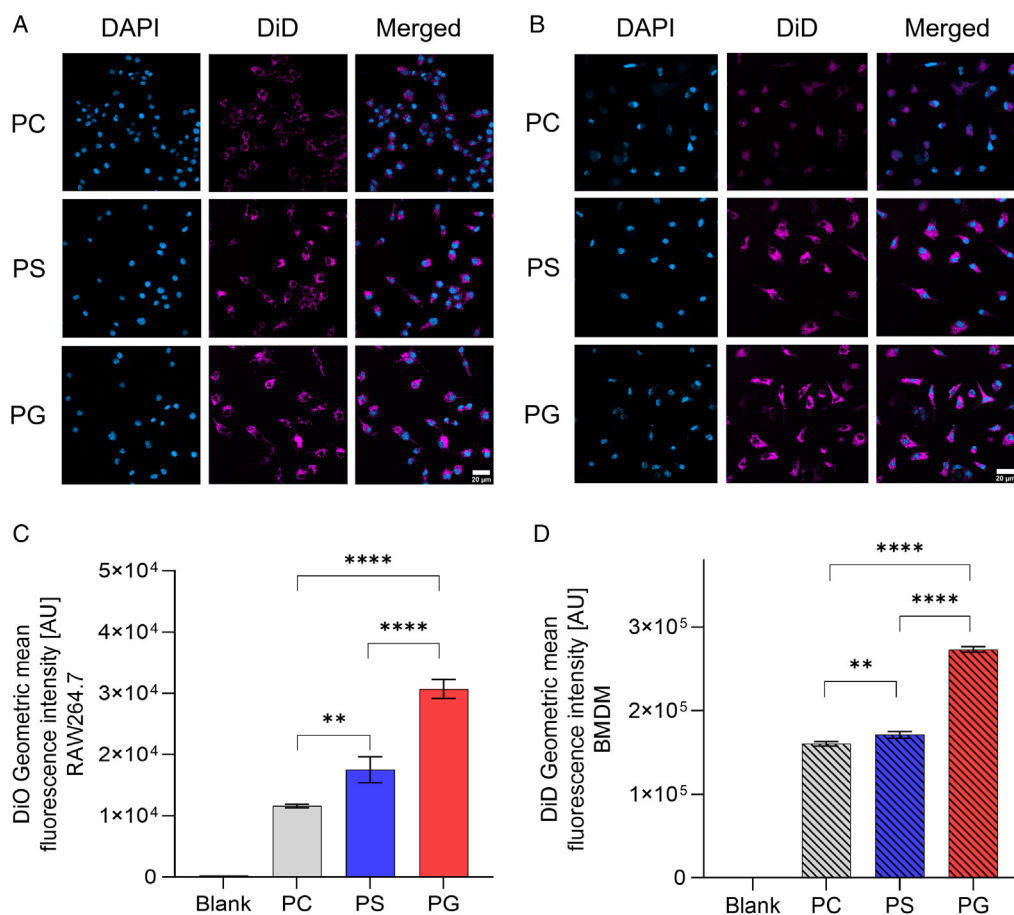


Figure 6. Liposomes uptake after 3 h of incubation followed by confocal microscopy on A) RAW264.7 cells (scale bar: 20 μ m) and on B) BMDM (scale bar: 20 μ m) and uptake by C) RAW264.7 cells and D) BMDM measured by flow cytometry. Data are represented as mean \pm SD ($n = 3$). Differences between groups were calculated by an ordinary one-way ANOVA combined with Sidak's multiple comparisons test after conducting the normality test (Shapiro–Wilk). Results are considered statistically significant if $p \leq 0.05$ (*), $p \leq 0.01$ (**), $p \leq 0.001$ (***), and $p \leq 0.0001$ (****).

their uptake efficiency by HeLa cells. By changing the lipid composition and specifically, using PG liposomes, either the amount or the identity of the proteins absorbed on vesicles surface can vary dramatically. In a previous study, the inclusion of DOPG lipid allowed for specific interactions between the lipid head group and the serum proteins which in turn led to a higher uptake.^[78] Similar results have been obtained on bone marrow dendritic cells: PG-containing liposomes have been reported to mediate a superior antigen-specific response compared with PS liposomes or cationic liposomes. It was found that PG liposomes attract complement proteins, especially C1q, from the circulation more efficiently than PS liposomes.^[66] However, further investigations are needed to elucidate the specific receptor involved in the uptake and its mechanism.

3. Conclusion

In the past decades, a manifold of different particle modifications to target macrophages has been proposed. Regrettably, it is still not well understood as to how each of these variables affects formulation performance. Inconsistent experimental conditions and missing controls in several studies from the literature (vide supra) lead to highly contradictory results. In this study, we have demonstrated the power of the DoE strategy for the development of liposomes and its ability to minimize the aforementioned disadvantages through a systematic, iterative screening. An extreme vertices design was used to determine the optimal combination of various lipids to deliver a desired response using a minimum number of experiments. Our DoE-led comprehensive particle characterization laid the foundation for the development of the most suited formulation (100 nm size and composed of 22 mol% of DOPG, 38 mol% of Chol, and 40 mol% of DOPC) for enhanced macrophage uptake. The results suggest that, although low rigidity of the phospholipid bilayer is beneficial for interaction with macrophages, it is seemingly not the only parameter to be taken into account, as other variables, such as Chol content, different NPLs, their concentration, and particle size, also critically affected the uptake. As a first step to test the translational potential of our systematic screening approach, the best candidate identified for the RAW264.7 cell line was confirmed with BMDM primary cells. For the first time, to our knowledge, our systematic approach allowed for the production of a suitable fluorescent liposome formulation efficiently taken up by both immortalized and primary macrophages. This study has set the stage for further in vivo studies to confirm the uptake of optimized liposomes by macrophages in different tissues, with the potential goal to modulate the function of this critical cell type in a wide range of inflammatory and immune pathologies.

4. Experimental Section

Materials and Methods: The phospholipids 1,2-dipalmitoyl-sn-glycero-3-phosphocholine (DPPC), 1,2-distearoyl-sn-glycero-3-phosphocholine (DSPC), 1,2-dioleoyl-sn-glycero-3-phosphocholine (DOPC), 1-palmitoyl-2-oleoyl-glycero-3-phosphocholine (POPC), 1,2-di-(9Z-octadecenoyl)-sn-glycero-3-phospho-(1'-rac-glycerol) (sodium salt) (DOPG), 1,2-distearoyl-sn-glycero-3-phospho-(1'-rac-glycerol) sodium salt (DSPG), and 1,2-dioleoyl-sn-glycero-3-phosphate sodium salt (DOPA) were kindly gifted by Lipoid (Ludwigshafen, Germany). 1,2-dipalmitoyl-sn-glycero-3-

phospho((ethyl-1',2',3'-triazole)triethyleneglycolmannose) (ammonium salt) (DPPA-PEG2-mannose), 1,2-dioctadecanoyl-sn-glycero-3-phosphate (sodium salt) (1,2-dioctadecanoyl-sn-glycero-3-phosphate (sodium salt) (DSPA), 1,2-dipalmitoyl-sn-glycero-3-phospho-L-serine (sodium salt) (DPPS), 1-hexadecanoyl-2-(9Z-octadecenoyl)-sn-glycero-3-phospho-L-serine (sodium salt) (POPS), L-alpha-PS (brain, porcine) (sodium salt) (Brain PS), and 1,2-dioleoyl-sn-glycero-3-phospho-L-serine (sodium salt) (DOPS) were purchased from Avanti Polar Lipids (Alabaster, USA). 3,3'-dioctadecylloxycarbocyanine perchlorate (DiO) and 1,1'-dioctadecyl-3,3,3',3'-tetramethylindodicarbocyanine, 4-chlorobenzenesulfonate salt (DiD) were bought from Thermo Fisher Scientific (Waltham, MA, USA). RAW264.7 cell line (Merck, ECACC 91062702, ATCC-TIB-71, *Mus musculus*-derived macrophages), HEK293 cell line (Merck, ECACC 85120602, human embryo kidney), penicillin/streptomycin solution (penicillin: 10 000 U mL⁻¹, streptomycin: 10 000 µg mL⁻¹), L-glutamine (200 mM), fetal bovine serum (FBS), cholesterol (Chol), 1,6-diphenyl-1,3,5-hexatriene (DPH), and palmitic acid were obtained from Merck (Darmstadt, Germany). Trifluoroacetic acid (TFA), ethylenediaminetetraacetic acid sodium salt (EDTA), Dulbecco's Modified Eagle Medium—high glucose (DMEM), Dulbecco's phosphate buffered saline (with and without calcium and magnesium) (DPBS), ROTI Histofix 4%, 4',6-diamidino-2-phenylindole dihydrochloride (DAPI), and propidium iodide were obtained from Carl Roth (Karlsruhe, Germany). All organic solvents (chloroform, methanol, acetonitrile, ethanol, and tetrahydrofuran [THF]) were obtained from Fisher Scientific (Schwerte, Germany).

Design of Experiment: The DoE approach allows to simultaneously investigate the effect of input variables and observe how these affect product quality. Mixture design was selected to optimize the proportions of lipids in liposome formulation to maximize a desired response using a minimum number of experiments. In this specific design, the response (i.e., the macrophages uptake expressed as geometric mean fluorescence intensity values from flow cytometry experiments) is a function of the proportions of the different lipid components in the mixture that must add up to one.^[79] As it was not desirable to have all constituents of the mixture varied in the ratio of zero to one, an extreme vertices design with lower and upper-bound constraints on the components was used. The constraints placed on the individual factors describe an irregular hyperpolyhedron.^[80] The vertices and centroids of this figure describe the 11 points of the experiment (see Figure S1, Supporting Information) used to estimate the response in the surface plot, where ranges of different geometric mean fluorescence intensity values obtained from flow cytometry experiments are divided in colored contour bands. Four independent DoE, in which neutral lipids (DOPC, POPC, DPPC, and DOPC + DSPC 50/50 mixture; with lower and upper bounds of 40 and 100 molar percentage, respectively) were formulated together with negatively charged lipids (DOPS, POPS, DPPS, Brain PS, respectively; with lower and upper bounds of 0 and 30 molar percentage, respectively) and cholesterol (Chol; with lower and upper bounds of 0 and 40 molar percentage, respectively), were conducted (see Table S1, Supporting Information). It is worth noting that each formulation contained a pair of neutral and negatively charged lipids having the same chain length and degree of unsaturation, resulting in a negligible hydrophobic mismatch, a phenomenon known to perturb the bilayer stability and membrane fluidity. Namely, DOPC was coformulated with DOPS, POPC, with POPS and the mixture DOPC/DSPC 50/50 with Brain PS. Each DoE consisted of 11 different liposome formulations conducted in triplicate. The model was fitted by a special cubic equation for three components using a statistical software (Minitab 18.1, Pennsylvania, USA). All the analyses together with a detailed description of the DoE are reported in Supporting Information (Figure S1 and S2; Tables S1–S13, Supporting Information).

Liposome Preparation: Liposomes containing the different lipid compositions were prepared by means of the film hydration method. Appropriate amounts of lipid stock solutions in chloroform and 0.1 mol% DiD or DiO were transferred into amber glass vials and the organic solvent was evaporated under a nitrogen stream until it dried. Both lipid dyes were routinely used for liposome research and they were reported to be non-exchangeable.^[81] Subsequently, solvent traces were removed by vacuum overnight. After hydration with DPBS (without calcium and magnesium,

to prevent aggregation of liposomes), the liposomal formulations was extruded five times through a 100 nm polycarbonate membrane (Whatman Nucleopore, Maidstone, UK) at room temperature (RT) for unsaturated lipid chains or above phase transition temperature for saturated lipid chains using a LIPEX extruder (Evonik, Canada). After liposome preparation, the lipid content of the different formulations was analyzed by a UHPLC-CAD-based approach (see Supporting Information) using a method previously developed in our group.^[82]

Size Evaluation and Zeta Potential: The hydrodynamic diameter and the polydispersity index (PDI) of the liposomes were determined by a Litesizer 500 (Anton Paar, Graz, Austria) equipped with a 175° backscatter angle detector and a semiconductor laser with $\lambda = 658$ nm. Briefly, the liposome formulations were diluted to a concentration of 100 μM , and 1 mL of the diluted dispersion was transferred into disposable semimicro cuvettes. After equilibrating the sample at 25 °C, measurement was carried out (6 runs \times 30 s for each sample). The zeta potential was determined by means of continuously monitored phase analysis light scattering (cmPALS) in an Omega cuvette (Anton Paar, Graz, Austria), where a refractive index of 1.33 and a viscosity of 0.89 mPa/s were set for the solvent. The intensity size distribution of the liposome was unimodal; therefore, the autocorrelation function was analyzed according to the cumulant method by the Kalliope™-software (Anton Paar).

Fluorescence Anisotropy: DPH was dissolved in THF to a concentration of 10 $\mu\text{g mL}^{-1}$ and stored at -20 °C, protected from light. For the analysis, 1 mL of liposome formulation (100 μM) was then mixed with DPH stock solution in a molar ratio of DPH: lipid (1:300). After 30 min incubation time at 37 °C and 300 rpm, 200 μL was transferred into a black 96-well plate (BRAND, Wertheim, Germany). After two additional shaking steps (orbital, 5 s), fluorescent anisotropy was determined by means of an Infinite 200 Pro F-Plex plate reader (Tecan, Männedorf, Switzerland) equipped with $\lambda_{\text{ex}} = 360 \pm 35$ nm and $\lambda_{\text{em}} = 430 \pm 20$ nm broad-pass filters at 37 °C and calculated using Equation (1).

$$r = \frac{G \cdot I_{\parallel} - I_{\perp}}{G \cdot I_{\parallel} + 2I_{\perp}} \quad (1)$$

where I_{\parallel} and I_{\perp} are the fluorescence intensities measured parallel and perpendicular to the vertically polarized exciting beam, and G (1.013) is an intrinsic parameter of the spectrometer.

Cell Culture: Semiadherent mouse monocyte macrophages (RAW264.7) were cultured at 37 °C in a humidified atmosphere containing 5% CO_2 in DMEM (4.5 g L^{-1} glucose and phenol red) supplemented with 1% v/v penicillin/streptomycin mixture, 1% v/v L-glutamine (200 nM), and 10% v/v FBS. After reaching 70–80% of confluence, the cells were detached by a cell scraper and used for further subcultivation. Adherent human embryonic kidney cells (HEK293) were cultured at 37 °C in a humidified atmosphere containing 5% CO_2 in DMEM (4.5 g L^{-1} glucose and phenol red) supplemented with 1% v/v penicillin/streptomycin mixture, 1% v/v of L-glutamine (200 nM), and 2% v/v FBS. After reaching 90% confluence, the cells were enzymatically detached and used for further subcultivation. Cells were regularly checked for the absence of mycoplasma.

BMDMs were isolated from the tibia, femur, and pelvic bones of 6–12-week-old C57BL/6J male mice according to a previously established protocol.^[27] Briefly, the marrow was flushed from the hind leg bones using BMDM media containing RPMI + Glutamine supplemented with 10% heat-inactivated FBS (FBS Gold, Gibco, Paisley, UK) and 100 IU mL^{-1} penicillin/streptomycin (P/S, Gibco, Paisley, UK). After thorough resuspension, the cells were filtered through a 100 μm pore mesh and incubated with 1 mL ammonium–chloride–potassium (ACK) Lysis Buffer (Gibco, Grand Island, NY, USA) to deplete erythrocytes. After washing, the cells were resuspended in BMDM media supplemented with 5 ng mL^{-1} recombinant mouse macrophage colony stimulating factor (mCSF, R&D Biosystems, Minneapolis, USA, 416-ML-500) and plated in nontreated cell culture Petri dishes (100 mm, Greiner Bio-One, St Gallen, Switzerland). A total of 20×10^6 hematopoietic stem cells per dish were cultured for 7 days at 37 °C, 5% CO_2 , with media exchange at culture day 4. At culture day 7, $\approx 1.5\text{--}3 \times 10^6$ cells per Petri dish were obtained.

Flow Cytometry: The uptake of different liposomal formulations was tested using three different cell types: RAW264.7, HEK293, and primary BMDMs. Briefly, 0.4×10^6 cells/well (RAW264.7) and 0.2×10^6 cells/well (HEK293) were seeded into 12-well plates (SPL Life Science) with 1 mL full-growth medium and cultured for 18 h at 37 °C, 5% CO_2 , to 90% confluence, whereas primary BMDMs were used at culture day 7 post-isolation, at a confluence of $\approx 2 \times 10^6$ cells/100 mm Petri dish. Prior to incubation with warm DPBS (with calcium and magnesium, to prevent detachment of the cells). Liposome stock dispersions were diluted in the following cell culture media at a final concentration of 100 μM : for RAW264.7 and HEK293, we used phenol red-free DMEM containing 4.5 g L^{-1} glucose supplemented with 1% v/v penicillin/streptomycin mixture, 1% v/v of L-glutamine (200 nM), and 2% v/v FBS, whereas for primary BMDMs, RPMI media supplemented with 10% FBS, 100 IU mL^{-1} P/S, and 5 ng mL^{-1} mCSF were used. All three cell types were then incubated for 180 min at 37 °C (100 rpm) with liposomal formulations. After incubation, the supernatant was removed, and cells were washed three times with ice-cold “FACS buffer” (DPBS without calcium and magnesium supplemented with 0.02 % w/v EDTA and 2% v/v FBS). Subsequently, RAW264.7 and HEK293 cells were detached with a cell scraper and pipetted into 1.5 mL reaction tubes. BMDM detachment was achieved by incubation of cells with 0.5% trypsin (Gibco, Paisley, UK, 25300-054) for 10 min at 37 °C, following which the enzyme was inactivated with BMDM media. After two additional washing steps, RAW264.7 and HEK293 cells were dispersed in 600 μL FACS buffer and transferred to the flow cytometer. BMDMs were additionally incubated on ice for 15 min with anti-CD16/32 (produced in house) to block the FC receptors and then incubated with the following reagents diluted in FACS buffer for 30 min at 4 °C in light-protected conditions: PE-Cy7 conjugated anti-mouse CD11b (clone M1/70, Biolegend, San Diego, CA, USA, catalogue number 101216), Brilliant Violet 711 conjugated anti-mouse CD45 (clone 30-F11, Biolegend, San Diego, CA, USA, catalogue number 103146), and cell viability dye eFluor 506 (Invitrogen, Rockford, IL, USA, catalogue number 65-0866-14). RAW264.7 and HEK293 cells were stained for 10 min with 50 $\mu\text{g mL}^{-1}$ propidium iodide diluted in ultrapure water for viability assessment. After antibody washout with $1 \times$ DPBS and prior to analysis, the cell dispersions were filtered through a 50 μm mesh (Hartenstein, Würzburg, Germany) to exclude clusters of cells. An LSR II SORP (BD Biosciences, Allschwil, Switzerland) reader was used to acquire the data for RAW264.7 and HEK293 cells, and an Attune NxT cytometer (Thermo Fisher Scientific, Rochester, NY, USA) was used for BMDM analysis. A minimum of 10 000 living cells per sample was recorded. The fluorescence intensity of the dye bound to the cell surface and/or internalized by the cells was assessed by means of a gating strategy shown in Supporting Information (Figure S3 and S4, Supporting Information). FlowJo software (version 10, Ashland, OR; USA) was used for data analysis and the geometric mean of the fluorescence intensity (GeoMean) measured by flow cytometry was chosen as output for the uptake of the different particles. GeoMean was proportional to the liposome/dye uptake where all the produced particles had the same fluorescence intensity and the same cell viability after incubation (See Figure S5 and S6 respectively, Supporting Information).

Confocal Microscopy: To observe the intracellular distribution and the fluorescence intensity of liposome formulations, we used confocal microscopy. For this purpose, 0.2×10^6 cells/well (RAW264.7) were seeded into 12-well plates (SPL Life Science) equipped with 1 glass coverslip per well. After 18 h, the cell culture medium was discarded, and wells were washed two times with DPBS (37 °C). In parallel, BMDMs were isolated and cultured on glass slides in 12-well plates (SPL Life Science) in BMDM media supplemented with 5 ng mL^{-1} mCSF at a density of 2.5×10^6 cells per well. Liposome stock dispersions with DiD were diluted in phenol red-free DMEM (for RAW264.7 cells)/BMDM media containing mCSF (for BMDMs) as described above and carefully pipetted onto the cells. Cells were then incubated with the liposomes for 180 min at 37 °C. After incubation, the supernatant was removed, and cells were washed three times with DPBS. Cells were then fixed with 1% paraformaldehyde (PFA, Merk Darmstadt, Germany) for 10 min at RT in light-protected conditions. After fixation and two washing steps with DPBS, nuclei staining was achieved by incubation of cells with DAPI (200 ng mL^{-1} , AppliChem, Darmstadt,

Germany) diluted in $1 \times$ DPBS. After additional two washing steps, cells were mounted with Mowiol 4-88 (Sigma-Aldrich, St Louis, MO, USA) and covered with glass slides. Imaging was conducted with a Zeiss LSM 800 (Carl Zeiss AG, Jena, Germany) confocal microscope, using a $40\times/1.3$ oil objective. For each sample, three pictures were acquired from three different fields of view.

Statistical Analysis: Results were expressed as mean \pm S.D. ($n=3$). Differences between groups were calculated by an ordinary one-way ANOVA combined with Sidak's multiple comparisons test after conducting normality test (Shapiro-Wilk). Results were considered statistically significant if $p \leq 0.05$ (*), $p \leq 0.01$ (**), $p \leq 0.001$ (***), and $p \leq 0.0001$ (****).

Supporting Information

Supporting Information is available from the Wiley Online Library or from the author.

Acknowledgements

The authors gratefully acknowledge funding from the UniBE ID Grants. G.L. kindly acknowledges the Swiss Multiple Sclerosis Foundation and the Ruth & Arthur Scherbarth Foundation. The authors acknowledge Dr. Urban Deutsch and the animal caretakers of the Theodor Kocher Institute for precious assistance in mouse colony maintenance. F.W., S.A., and P.L. thank the staff of the Flow Cytometry Core Facility of the Medical Faculty, Department for BioMedical Research (DBMR), University of Bern, Switzerland, for their valuable technical support. S.A. would like to acknowledge Silvia Faieta from BSP Pharmaceuticals SpA, Italy, for her precious revisions of the Design of Experiment sections.

Conflict of Interest

The authors declare no conflict of interest.

Data Availability Statement

Data available on request from the authors.

Keywords

bone marrow-derived macrophages, design of experiments, liposomes, macrophages, quality by designs, RAW264.7, targeting

Received: November 30, 2020

Revised: January 5, 2021

Published online: February 3, 2021

- [1] P. J. Murray, T. A. Wynn, *Nat. Rev. Immunol.* **2011**, *11*, 723.
- [2] S. Gordon, *Nat. Rev. Immunol.* **2003**, *3*, 23.
- [3] F. Tacke, *J. Hepatol.* **2017**, *66*, 1300.
- [4] V. Bagalkot, J. A. Deiliulis, S. Rajagopalan, A. Maiseyev, *Adv. Drug Deliv. Rev.* **2016**, *99*, 2.
- [5] C. T. Ingkut, A. J. Sorrin, T. Kuruppu, S. Vig, J. Cicalo, H. Ahmad, H. C. Huang, *Nanomaterials* **2020**, *10*, 190.
- [6] N. M. La-Beck, A. A. Gabizon, *Front. Immunol.* **2017**, *8*, 416.
- [7] T. Ishida, S. Kashima, H. Kiwada, *J. Control. Release* **2008**, *126*, 162.
- [8] A. Gao, X. L. Hu, M. Saeed, B. F. Chen, Y. P. Li, H. J. Yu, *Acta Pharmacol. Sin.* **2019**, *40*, 1129.
- [9] C. Kelly, C. Jefferies, S.-A. Cryan, *J. Drug Deliv.* **2011**, *2011*, 727241.
- [10] N. Wang, M. Chen, T. Wang, *J. Control. Release* **2019**, *303*, 130.
- [11] I. Shlomovitz, M. Speir, M. Gerlic, *Cell Commun. Signal.* **2019**, *17*, 139.
- [12] Z. G. Ramirez-ortiz, W. F. P. Iii, A. Prasad, M. H. Byrne, C. J. Blanchette, A. D. Luster, N. Hacohen, J. El, T. K. Means, *Nat. Immunol.* **2014**, *14*, 917.
- [13] G. Lemke, *Nat. Rev. Immunol.* **2019**, *19*, 539.
- [14] R. Chaurio, C. Janko, L. Muñoz, B. Frey, M. Herrmann, U. Gaip, *Molecules* **2009**, *14*, 4892.
- [15] H. Pichler, A. Emmerstorfer-Augustin, *Methods* **2018**, *147*, 50.
- [16] M. E. Klein, S. Mauch, M. Rieckmann, D. G. Martínez, G. Hause, M. Noutsias, U. Hofmann, H. Lucas, A. Meister, G. Ramos, H. Loppnow, K. Mäder, *Nanomed. Nanotechnol. Biol. Med.* **2020**, *23*, 102096.
- [17] V. Haucke, G. Di Paolo, *Curr. Opin. Cell Biol.* **2007**, *19*, 426.
- [18] T. Keler, V. Ramakrishna, M. W. Fanger, *Expert Opin. Biol. Ther.* **2004**, *4*, 1953.
- [19] M. Xiong, Q. Lei, X. You, T. Gao, X. Song, Y. Xia, T. Ye, L. Zhang, N. Wang, L. Yu, *J. Microencapsul.* **2017**, *34*, 513.
- [20] L. X. Yu, G. Amidon, M. A. Khan, S. W. Hoag, J. Polli, G. K. Raju, J. Woodcock, *AAPS J.* **2014**, *16*, 771.
- [21] A. Jain, P. Hurkat, S. K. Jain, *Chem. Phys. Lipids* **2019**, *224*, 104764.
- [22] J. W. Shreffler, J. E. Pullan, K. M. Dailey, S. Mallik, A. E. Brooks, *Int. J. Mol. Sci.* **2019**, *20*, 6056.
- [23] Y. T. Goo, S. Y. Park, B. R. Chae, H. Y. Yoon, C. H. Kim, J. Y. Choi, S. H. Song, Y. W. Choi, *Int. J. Pharm.* **2020**, *585*, 119483.
- [24] K. Mulia, A. C. Singarimbun, E. A. Krisanti, *Int. J. Mol. Sci.* **2020**, *21*, 873.
- [25] S. Sieber, P. Grossen, P. Uhl, P. Detampel, W. Mier, D. Witzigmann, J. Huwyler, *Nanomed. Nanotechnol. Biol. Med.* **2019**, *17*, 82.
- [26] M. Guo, A. Härtlova, B. D. Dill, A. R. Prescott, M. Gierliński, M. Trost, *Proteomics* **2015**, *15*, 3169.
- [27] G. Locatelli, D. Theodorou, A. Kendirli, M. J. C. Jordão, O. Staszewski, K. Phulphagar, L. Cantuti-Castelvetri, A. Dagkalis, A. Bessis, M. Simons, F. Meissner, M. Prinz, M. Kerschensteiner, *Nat. Neurosci.* **2018**, *21*, 1196.
- [28] C. Kelly, C. Jefferies, S.-A. Cryan, *J. Drug Deliv.* **2011**, *2011*, 727241.
- [29] A. Gauthier, A. Fisch, K. Seuwen, B. Baumgarten, H. Ruffner, A. Aebi, M. Rausch, F. Kiessling, M. Bartneck, R. Weiskirchen, F. Tacke, G. Storm, T. Lammers, M. G. Ludwig, *Biomaterials* **2018**, *178*, 481.
- [30] T. Geelen, S. Y. Yeo, L. E. M. Paulis, L. W. E. Starmans, K. Nicolay, G. J. Strijkers, *J. Nanobiotechnol.* **2012**, *10*, 37.
- [31] S. Khadke, C. B. Roces, A. Cameron, A. Devitt, Y. Perrie, *J. Control. Release* **2019**, *307*, 211.
- [32] Y. Kono, S. Gogatsubo, T. Ohba, T. Fujita, *Drug Deliv.* **2019**, *26*, 935.
- [33] T. Harel-Adar, T. Ben Mordechai, Y. Amsalem, M. S. Feinberg, J. Leor, S. Cohen, *Proc. Natl. Acad. Sci.* **2011**, *108*, 1827.
- [34] Z. Wu, H. M. Ma, T. Kukita, Y. Nakanishi, H. Nakanishi, *J. Immunol.* **2010**, *184*, 3191.
- [35] S.-H. Park, S.-G. Oh, J.-Y. Mun, S.-S. Han, *Colloids Surf., B* **2005**, *44*, 117.
- [36] D. M. Cauvi, D. Hawisher, P. R. Dores-Silva, R. E. Lizardo, A. De Maio, *FASEB J.* **2019**, *33*, 2995.
- [37] L. da Costa Loureiro, L. da Costa Loureiro, E. A. Gabriel-Junior, F. A. Fambuzi, C. Fontanari, H. Sales-Campos, F. G. Frantz, L. H. Faccioli, C. A. Sorgi, *Mol. Immunol.* **2020**, *122*, 163.
- [38] T. M. Allen, G. A. Austin, A. Chonn, L. Lin, K. C. Lee, *Biochim. Biophys. Acta – Biomembr.* **1991**, *1061*, 56.
- [39] H. H. Spanjer, M. van Galen, F. H. Roerdink, J. Regts, G. L. Scherphof, *Biochim. Biophys. Acta – Biomembr.* **1986**, *863*, 224.
- [40] T. Mazumdar, K. Anam, N. Ali, *J. Parasitol.* **2005**, *91*, 269.
- [41] O. Bakouche, D. Gerlier, *Immunology* **1986**, *58*, 507.

- [42] C. R. Miller, B. Bondurant, S. D. McLean, K. A. McGovern, D. F. O'Brien, *Biochemistry* **1998**, *37*, 12875.
- [43] D. Papahadjopoulos, H. K. Kimelberg, *Prog. Surf. Sci.* **1974**, *4*, 141.
- [44] W. W. Sułkowski, D. Pentak, K. Nowak, A. Sułkowska, *J. Mol. Struct.* **2005**, *744–747*, 737.
- [45] A. Katragadda, R. Bridgman, G. Betageri, *Cell. Mol. Biol. Lett.* **2000**, *5*, 483.
- [46] A. J. van Houte, H. Snippe, M. G. Schmitz, J. M. Willers, *Immunology* **1981**, *44*, 561.
- [47] Y. Nakano, M. Mori, H. Yamamura, S. Naito, H. Kato, M. Taneichi, Y. Tanaka, K. Komuro, T. Uchida, *Bioconjug. Chem.* **2002**, *13*, 744.
- [48] T. M. Allen, G. A. Austin, A. Chonn, L. Lin, K. C. Lee, *Biochim. Biophys. Acta – Biomembr.* **1991**, *1061*, 56.
- [49] C. Koo, M. E. Wernet-Hammond, Z. Garcia, M. J. Malloy, R. Uauy, C. East, D. W. Bilheimer, R. W. Mahley, T. L. Innerarity, *J. Clin. Invest.* **1988**, *81*, 1332.
- [50] M. Brundert, J. Heeren, M. Bahar-Bayansar, A. Ewert, K. J. Moore, F. Rinninger, *J. Lipid Res.* **2006**, *47*, 2408.
- [51] C. Barnier-Quer, A. Elsharkawy, S. Romeijn, A. Kros, W. Jiskoot, *Pharmaceutics* **2013**, *5*, 392.
- [52] H. S. Kruth, *Curr. Pharm. Des.* **2013**, *19*, 5865.
- [53] W. Hofkens, L. C. Grevers, B. Walgreen, T. J. De Vries, P. J. M. Leenen, V. Everts, G. Storm, W. B. Van Den Berg, P. L. Van Lent, *J. Control. Release* **2011**, *152*, 363.
- [54] J. Westman, S. Grinstein, P. E. Marques, *Front. Immunol.* **2020**, *10*, 3030.
- [55] K. Wong, P. A. Valdez, C. Tan, S. Yeh, J. A. Hongo, W. Ouyang, *Proc. Natl. Acad. Sci. U. S. A.* **2010**, *107*, 8712.
- [56] S. A. Johnstone, D. Masin, L. Mayer, M. B. Bally, *Biochim. Biophys. Acta – Biomembr.* **2001**, *1513*, 25.
- [57] F. Giulimondi, L. Digiaco, D. Pozzi, S. Palchetti, E. Vulpis, A. L. Capriotti, R. Z. Chiozzi, A. Laganà, H. Amenitsch, L. Masuelli, G. Peruzzi, M. Mahmoudi, I. Screpanti, A. Zingoni, G. Caracciolo, *Nat. Commun.* **2019**, *10*, 3686.
- [58] S. Palchetti, D. Pozzi, A. L. Capriotti, G. La Barbera, R. Z. Chiozzi, L. Digiaco, G. Peruzzi, G. Caracciolo, A. Laganà, *Colloids Surf., B* **2017**, *153*, 263.
- [59] X. Yan, G. L. Scherphof, J. A. A. M. Kamps, *J. Liposome Res.* **2005**, *15*, 109.
- [60] A. Gibbons, D. Padilla-Carlin, C. Kelly, A. J. Hickey, C. Taggart, N. G. McElvaney, S.-A. Cryan, *Pharm Res.* **2011**, *28*, 2233.
- [61] N.-T. Thi Nguyen, S. Yun, D. W. Lim, E. K. Lee, *Prep. Biochem. Biotechnol.* **2018**, *48*, 522.
- [62] J. R. Silvius, in *Lipid-Protein Interactions* (Eds: P. C. Host, O. H. Griffith), Wiley, New York, **1982**, p. 239.
- [63] A. K. Azad, M. V. S. Rajaram, L. S. Schlesinger, *J. Cytol. Mol. Biol.* **2014**, *1*, 1000003.
- [64] L. Martinez-Pomares, S. A. Linehan, P. R. Taylor, S. Gordon, *Immunobiology* **2001**, *204*, 527.
- [65] H. H. Tuson, G. K. Auer, L. D. Renner, M. Hasebe, C. Tropini, M. Salick, W. C. Crone, A. Gopinathan, K. C. Huang, D. B. Weibel, *Mol. Microbiol.* **2012**, *84*, 874.
- [66] N. Benne, J. van Duijn, F. Lozano Vigario, R. J. T. Lebourg, P. van Veelen, J. Kuiper, W. Jiskoot, B. Slütter, *J. Control. Release* **2018**, *291*, 135.
- [67] K. Kuronuma, H. Mitsuzawa, K. Takeda, C. Nishitani, E. D. Chan, Y. Kuroki, M. Nakamura, D. R. Voelker, *J. Biol. Chem.* **2009**, *284*, 25488.
- [68] N. Yanasarn, B. R. Sloat, Z. Cui, *Mol. Pharm.* **2011**, *8*, 1174.
- [69] S. Mauch, M. Rieckmann, D. G. Martínez, G. Hause, M. Noutsias, U. Hofmann, H. Lucas, A. Meister, G. Ramos, H. Loppnow, K. Mäder, *Nanomed. Nanotechnol., Biol. Med.* **2020**, *23*, 102096.
- [70] M. Schwegler, A. M. Wirsing, A. J. Dollinger, B. Abendroth, F. Putz, R. Fietkau, L. V. Distel, *Biol. Cell* **2015**, *107*, 372.
- [71] F. Ahsan, I. P. Rivas, M. A. Khan, A. I. Torres Suárez, *J. Control. Release* **2002**, *79*, 29.
- [72] S. Chono, T. Tanino, T. Seki, K. Morimoto, *J. Drug Target.* **2006**, *14*, 557.
- [73] S. Chono, T. Tanino, T. Seki, K. Morimoto, *J. Pharm. Pharmacol.* **2007**, *59*, 75.
- [74] R. Toita, E. Shimizu, J. H. Kang, *Chem. Commun. (Cambridge, U.K.)* **2020**, *56*, 8253
- [75] Q. Zhang, G. Liao, D. Wei, T. Nagai, *Int. J. Pharm.* **1998**, *164*, 21.
- [76] M. Henriksen-Lacey, A. Devitt, Y. Perrie, *J. Control. Release* **2011**, *154*, 131.
- [77] H. Epstein-Barash, D. Gutman, E. Markovsky, G. Mishan-Eisenberg, N. Koroukhov, J. Szebeni, G. Golomb, *J. Control. Release* **2010**, *146*, 182.
- [78] K. Yang, B. Mesquita, P. Horvatovich, A. Salvati, *Acta Biomater.* **2020**, *106*, 314.
- [79] R. D. Snee, *Commun. Stat. – Theory Methods* **1979**, *8*, 303.
- [80] R. D. Snee, D. W. Marquardt, *Technometrics* **1974**, *16*, 399.
- [81] M. G. Honig, R. I. Hume, *J. Cell Biol.* **1986**, *103*, 171.
- [82] F. Weber, L. Rahnfeld, P. Luciani, *Talanta* **2020**, *121320*.